

§1. Darcy's Law. Conservation Equations. Effective Forces. The seepage of liquid and gas through porous media have been investigated for more than two centuries. Mathematical analysis of the seepage phenomenon is founded on the law experimentally observed by the French engineer Darcy in 1856 [1]. This law establishes the proportionality between seepage rate (the volume of liquid or gas passing through a unit area of cross section of a porous medium per unit time) and the projection of the pressure gradient on the normal to this cross section.

If  $\bar{v}$  is the vector of the seepage rate,  $k$  is the "permeability," which has the dimensions of area,  $\mu$  is the viscosity of the liquid or gas, and  $p$  is pressure, Darcy's law assumes the form

$$\bar{v} = -\frac{k}{\mu} \bar{\nabla} p; \quad (1.1)$$

$$\bar{\nabla} = \bar{i} \frac{\partial}{\partial x} + \bar{j} \frac{\partial}{\partial y} + \bar{k} \frac{\partial}{\partial z}.$$

The permeability is usually expressed in millidarcies (1 mDc =  $10^{-11}$  cm<sup>2</sup>). The permeability of beds containing oil and gas is of the order of tens or hundreds of millidarcies. In coal seams, the permeability is  $10^{-13}$ - $10^{-15}$  cm<sup>2</sup> in the vicinity of a working.

Under large pressure gradients, laboratory tests sometimes correspond better to the more complex relationship (the generalized Darcy law for "turbulent flows")

$$-\bar{\nabla} p = \frac{\mu}{k} \bar{v} + \frac{\rho v}{L} \bar{v}, \quad (1.2)$$

where  $\rho$  is the density and  $L$  is a coefficient with the dimension of length.

Laboratory tests to determine permeability are usually conducted on cylindrical specimens. A schematic diagram of such a test is shown in Fig. 1, where  $p_I$  and  $p_{II}$  are the pressures in reservoirs I and II at the ends of the specimen.

Darcy's law is always better confirmed under a steady-state uniform flow of liquid and moderate pressure gradients (see Fig. 1). The pressure gradient is constant along the length of the specimen during the seepage of a liquid, and increases in the direction of flow during the seepage of a gas (Fig. 2).

For large pressure gradients, relationship (1.2) or even the more complex relationship between pressure gradient and seepage rate is found to be more valid only for specific structures of the soil particles.

If the equation expressing the law of mass conservation is combined with relationship (1.1) or (1.2), it is possible to obtain a differential equation to determine the pressure field and seepage-rate field.

Calculations of the steady-state flows of water, petroleum, and gas in layers of porous rock under the most diverse conditions indicate varying degrees of agreement with field measurements and confirm that Darcy's law or its generalization is a reliable basis of seepage theory [1].

In the 1970s, however, measurements of the pressure that develops under nonsteady regimes of the seepage flows of petroleum and water, which are a consequence of marked changes in flow rate in individual wells (for a large-scale oil reservoir), indicated a striking qualitative discrepancy between computational data based on Darcy's law and field measurements

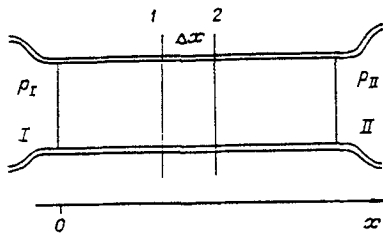


Fig. 1

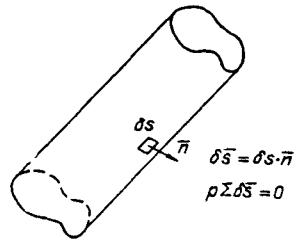


Fig. 2

[2, 3]. It was observed, for example, that propagation of disturbances in seepage flow occurs at a well defined and very small rate (of the order of units of centimeters per second). At the same time, theoretical studies conducted with nonsteady flows of mixtures of coal particles and gas with a high concentration indicated that the force of interaction between the coal and gas in any case it is impossible to reduce to hydrodynamic resistance forces, which depend on the difference in the velocities of the coal and gas (for example, to Stokes law), and that these forces are normally almost negligibly small as compared with "Archimedes force," which is caused by the pressure gradient in a wave [4].

Let  $m$  be the porosity (the volume of pores per unit volume of soil), and  $\omega$  be the clearance (the cross-sectional area of pores per unit cross-sectional area of soil). For the analysis, the element of soil volume under consideration should always be sufficiently large to contain a large number of pores for a statistically reliable averaging process in determining  $m$  and  $\omega$ . If  $\omega = m$  for a cross section of any orientation, the porosity is uniform. The simplest isotropic structure of a porous medium is a structure with a uniformly distributed porosity.

Porosity may differ in space not only in magnitude, but also in the quantity and size and shape of the pores which are required during averaging to determine a reliable value of the clearance  $\omega$ , the average velocity  $u$  in the apertures and the average pressure  $p$  in the pores across a section at a site with unit cross-sectional area.

During seepage, the liquid (gas) flows through an interconnected system of pores.

Forces of interaction between the liquid (gas) and soil particles during seepage are always three-dimensional. We will designate the force acting in a unit volume of soil due to the liquid (gas) against the soil particles by the letter  $\bar{\mathcal{P}}$ . When  $\bar{\mathcal{P}}$  appears hereinafter, it is precisely the structure of the porous space that plays the decisive role in formulating the character of the seepage flow.

For simplicity, we will first dwell on study of a porous medium with a uniformly distributed porosity over the entire space under consideration in both magnitude and structure.

Let us set up the equations of mass conservation and the variation in the amount of movement and the energy equation for the seepage of a gas. Then, we will concentrate on analysis of the nature of the forces of interaction between the soil particles and seeping liquid (gas).

The equation of mass conservation for the liquid (gas) is derived from obvious considerations of the balance between the amount of liquid flowing into an element of soil volume and the increase in mass of this volume. For an absolutely rigid soil framework and when  $m = \text{const}$ , the equation of mass conservation is:

$$\frac{d \ln \rho}{dt} + \bar{\nabla} \cdot \bar{u} = 0, \quad (1.3)$$

where  $\bar{u}$  is the average actual velocity in the pores,  $\rho$  is the density of the fluid (gas),  $\bar{\nabla} = m\bar{u}$ , and  $d/dt = \partial/\partial t + \bar{u} \cdot \bar{\nabla}$ .

Let us now set up the equation of variation in the amount of motion. Elements of the volume of the porous medium in conservation equations should always be reasonably large in comparison with the dimensions of the pores and contain the amount of resistance force applied to the mass of liquid (gas) per unit of soil. In our case - one-dimensional flow - let us designate the projection of this force in the positive direction of the  $x$  axis by  $\mathcal{P}$  (see Fig. 1).

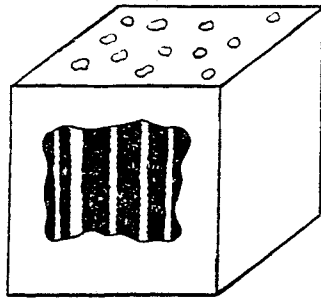


Fig. 3

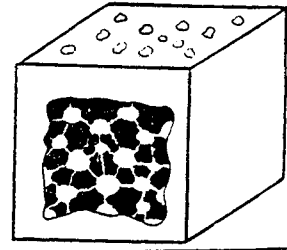


Fig. 4

Let us refer back to the experiment (see Fig. 1). Let there be a steady-state seepage of liquid ( $p_I$  and  $p_{II}$  are the constant static pressures in chambers I and II). Since  $\rho = \text{const}$ , the seepage rate is constant over the length of the specimen. The flow is uniform, and there are no inertial forces of the averaged flow. The hydrostatic resistance force  $-\mathcal{P}$  is equated to the pressure gradient in the apertures of the sections. In an element of the cross-sectional area, which is equal to 1 and which is included between the planes of cross sections 1 and 2 at a distance  $\Delta x$  one from the other (see Fig. 1),

$$-\mathcal{P}\Delta x = m(p_2 - p_1),$$

where  $p_1$  and  $p_2$  are the average pressures in the apertures of these sections, so that

$$\mathcal{P} = -m \frac{\partial p}{\partial x}. \quad (1.4)$$

If Darcy's law (1.1) is valid, the force  $\mathcal{P}$  in this case will be:

$$\mathcal{P}_d = \frac{m^2 \mu u}{\kappa}. \quad (1.5)$$

For nonuniform and nonsteady flows, it is obviously assumed that the inertial forces are always negligibly small in comparison with the hydrostatic resistance force, and it is assumed that the resistance force is always equated to the force of the pressure gradient alone. This is based on comparison of the inertial force  $\rho m(du/dt)$  for the mass of liquid included in the unit of soil volume and the force  $\mathcal{P}_d$ . Let us compare the values of  $du/dt$  and  $\mathcal{P}_d/\rho m = \mu u/\kappa \rho$ . At an absolute temperature  $T = 300^\circ\text{K}$ ,  $\rho \approx 1 \text{ g/cm}^3$  and  $\mu \approx 10^{-2} \text{ g/(cm}\cdot\text{sec)}$  for water and petroleum\*; and,  $\mu = 10^{-4} \text{ g/(cm}\cdot\text{sec)}$  and  $\rho \approx 10^{-2} \text{ g/cm}^3$  for a gas (when  $p = 1 \text{ MPa}$ ). Let us use typical values for seepage in porous rock:  $m = 0.1$ ,  $\kappa = 10^{-9} \text{ cm}^2$  (100 mDc),  $v = 10^{-2} \text{ cm/sec}$ , and  $u = 0.1 \text{ cm/sec}$ . Then,  $\mu u/\kappa \rho = 10^5 \text{ cm/sec}^2$ . If the seepage rate doubles after 100 sec for a nonsteady flow when  $u = 0.1 \text{ cm/sec}$ , the acceleration  $du/dt$  will be of the order of  $10^{-3} \text{ cm/sec}^2$ , and the inertial force will then be  $10^8$  times smaller than the resistance force. Even if the acceleration is very high (of the order of  $1 \text{ cm/sec}^2$ ), the inertial forces will still be  $10^5$  times smaller than  $\mathcal{P}_d$ .

This conclusion is directly associated with the method by which the experiments are carried out to determine the permeability; this method is based on considerations of dimensionality on the implied assumption that the forces of interaction between the seepage flow and soil framework are completely described by hydrodynamic friction forces dependent on the Reynolds number, i.e., on the seepage rate, viscosity, and density of the liquid (gas), and certain geometric dimensions.

This statement is associated with specific but not always clearly expressed notions concerning the structure of the porous space. It is assumed that the "system of porous channels is hydrodynamically equivalent to a system of complexly coupled tubes" (see [5, p. 10]).

For such a medium consisting of a system of capillary tubes, the forces acting on a flowing liquid (gas) due to the capillary walls is actually reduced to only hydrodynamic friction forces (tangential stresses on the walls of the tubes). The pressure forces on the walls of the tubes, the cross section of which is smooth and varies slightly with length, are balanced

\*The values are given in the CGS system, which is preferred by the author.

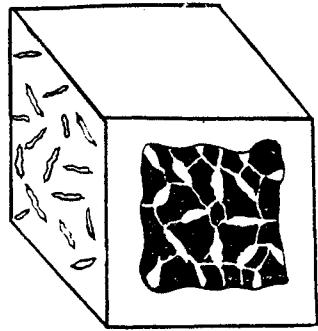


Fig. 5



Fig. 6

one with the other for each cylindrical element of tube, as if its section does not have shape, and do not therefore yield any component of force in the direction of the seepage flow (Fig. 2, where  $\delta s = n \cdot \delta s$  is an oriented surface element, and  $n$  is a unit vector of the normal). In this case, these tubes may be as complexly curved and seemingly intertwined as is desired. Darcy's law  $\mathcal{P} = \mathcal{P}_i = \mathcal{P}_a$  is always valid for this medium. The simplest model of this medium is shown in Fig. 3. It is more difficult to represent this medium with a uniform porosity, i.e. similar clearance in any direction.

Actual porous media have an entirely different structure. This structure is either solid grains cemented one to the other (sandstones) or fissured pores (limestones), some of whose pores are cracks of different sizes and orientations, or pores in coals and artificial materials. In all these cases, the porous space is a chain of reservoirs (pores) of different shape, but relatively large volume, which are interconnected by very fine slits, the section of which is usually many hundreds and thousands of times smaller than the section of the pores. The volume of these slits is negligibly small in comparison with the volume of the pores. Schematically, such a medium takes on the form presented in Figs. 4 and 5. For such a medium, the hydrostatic force of interaction between the seeping liquid (gas) and soil skeleton  $\bar{\mathcal{P}} = \bar{\mathcal{P}}_p + \bar{\mathcal{P}}_i$  is reduced primarily to the sum of pressure forces  $\bar{\mathcal{P}}_p$  ("Archimedes force") and the hydrodynamic friction forces  $\bar{\mathcal{P}}_i$ , which are insignificantly small in comparison with the pressure forces [6].

Corresponding sections of a pore close to the site of a cross section for two principally different structures with the same clearance are shown in magnified form in Figs. 6 and 7. In the cross sections, the clearance area is the same (the porosity is the same), but the projection of the cut portion of the surface of the pore on the area of the section is completely different for these structures. It is equal to zero in Fig. 7, and is nearly equal to the cross-sectional area of the pore in Fig. 6. When we examine the surface of a sandstone or limestone specimen, therefore, we do not see pores, and it appears continuous, while its surface is only slightly roughened.

If the pores are a system of capillary tubes, the projection of the pressure forces of the liquid (gas), which is applied to the soil framework, is equal to zero in the sections of the pores, and is almost equal to  $pm$  per unit area of section for a real structure.

Let us examine the flow of a liquid (gas) in a pore for small  $M$  numbers. We have  $p + \rho w^2/2 = p_0$ , where  $w$  is the velocity,  $p$  is the static pressure, and  $p_0$  is the stagnation pressure (total pressure) at a given point in the flow, and the number  $M = w/a$ , where  $a$  is the speed of sound. Everywhere in the pore, with the exception of small volumes near the inlet to narrow connected slits, the velocity  $w$  is close to  $u$ , i.e., very small (of the order of fractions of centimeters per second), so that the velocity head  $\rho w^2/2$  is negligibly small as compared with the pressure  $p$  and  $p \approx p_0$ . In the narrow connected slits, however, the velocity  $w$  is hundreds and thousands of times greater than  $u$ , and  $w$  can easily reach values of many meters per second. The velocity head  $\rho w^2/2$  becomes significant, for example,  $\rho = 1 \text{ g/cm}^3$ ,  $w = 200 \text{ cm/sec}$ , and  $\rho w^2/2 = 2 \cdot 10^4 \text{ g/(cm} \cdot \text{sec)} = 0.002 \text{ MPa}$  for water.

On exiting from a slit into the next pore, the velocity head is only partially restored in the form of pressure (this depends on the shape of the slit). When the slit is flat, this head is completely lost, i.e., is not transformed into pressure. For the slit shape shown in Fig. 8, only some of the velocity head is lost. On passing through each neighboring pair of pores, the next portion of the velocity head is lost, and the pressure  $p$  is correspondingly



Fig. 7

Fig. 8

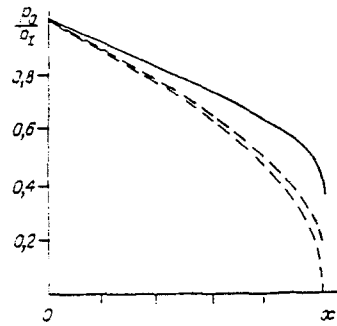


Fig. 9

reduced without a corresponding increase in  $u$ . The velocity  $u$  increases due only to a corresponding decrease in density. This is also a throttling phenomenon. For an ideal gas, this means a pressure loss  $p$  without a change in its absolute temperature  $T$ , i.e., its internal energy.

The pressure force of the gas in section 1 (see Fig. 1), which is applied to the soil framework in this porous medium at a site with an area equal to unity is  $pm(1 - \epsilon^2)$  when  $\epsilon^2 \ll 1$ , and at the same site at a distance  $\Delta x$  it is  $-m(p + \partial p/\partial x \Delta x)(1 - \epsilon^2)$ . Consequently, the hydrostatic force  $\mathcal{P}_p$ , which is caused by the pressure gradient of the "Archimedes force" and which falls on a unit volume of soil, will be

$$\mathcal{P}_p = -m \frac{\partial p}{\partial x} (1 - \epsilon^2). \quad (1.6)$$

The forces of hydrodynamic friction, which are caused by tangential stresses on the surfaces of the pores and narrow slits during laminar flow can be represented as

$$\mathcal{P}_\tau = \frac{m^2 \mu u}{\chi}, \quad (1.7)$$

where  $\chi$  has the dimensions of area, or

$$\mathcal{P}_\tau = \frac{m^2 \mu u}{\chi} + \frac{m^2 u^2 \rho}{\lambda}, \quad (1.8)$$

where  $\lambda$  has the dimension of length for turbulent flow.

The forces acting on a volume of soil having a cross-sectional area of unity between planes at a distance  $\Delta x$  from one another (see Fig. 1) will be the forces of gas pressure in the sections of the pores in these planes, which are equal to  $-m(\partial p/\partial x)\Delta x$ , and the hydrostatic forces  $-(\mathcal{P}_p + \mathcal{P}_\tau)\Delta x$ . The equation of the change in the amount of pressure in the projection on the  $x$  axis for a laminar flow will be:

$$\rho m \frac{du}{dt} = -m \frac{\partial p}{\partial x} + m(1 - \epsilon^2) \frac{\partial p}{\partial x} - \frac{m^2 \mu u}{\chi}$$

or

$$\rho \frac{du}{dt} + \epsilon^2 \frac{\partial p}{\partial x} + \frac{\mu m u}{\chi} = 0. \quad (1.9)$$

For a uniform flow, however, (1.5) should be such that

$$\frac{\partial p}{\partial x} + \frac{\mu m u}{\chi} = 0.$$

Consequently [6],

$$\kappa = \varepsilon^2 \chi. \quad (1.10)$$

In the case of "turbulent" flow,

$$\frac{\rho}{\varepsilon^2} \cdot \frac{du}{dt} + \frac{\partial p}{\partial x} + \frac{\mu mu}{\kappa} + \rho \frac{m^2 u^2}{L} = 0, \quad (1.11)$$

where

$$L = \varepsilon^2 \lambda. \quad (1.12)$$

If the thickness of the surface of the film and the thickness of the layer along the boundary in the narrow connected slits is neglected, the constant  $\varepsilon$ , as is apparent, is a geometric quantity (see below), which is related to the ratio of projections of the narrowest sections of the slits at the outlet from pores intersected by a given section with a clearance in the plane of this section.

If  $\varepsilon^2$  is of the order of  $10^{-7}$ - $10^{-9}$ , the internal forces are comparable to the resistance forces, and may even exceed them, as the above-cited assessments indicate.

To explain this matter, let us visualize the following experiment. Let a very light hollow body be immersed in a liquid and held in equilibrium by the tension  $T$  on a filament. Let us increase the filament tension to the limit at which the motion of the body becomes uniform. The difference between the tensile force of the filament and Archimedes force  $\Phi_A$  will then be equal to the resistance force. If the observer does not know the presence of the Archimedes force, i.e., assumes, for example, that the body is in motion in the gas, he will assume that the large tensile force of the filament is associated with the large resistance of the body, and obtain  $T = \mu V / \kappa$ , where  $V$  is the volume of the body,  $\mu$  is the viscosity, and  $u$  is the velocity that determines the coefficient  $\kappa$ , which assumes the dimensions of area, if the resistance is considered proportional to the velocity and viscosity. Very small values are obtained for  $\kappa$ . In effect, it would be necessary to write:  $T - \Phi_A = \mu V / \chi$ . If  $T - \Phi_A = \varepsilon^2 T$ , then  $\kappa = \varepsilon^2 \chi$ . It is as though  $\kappa$  or  $\chi$  are used indifferently for uniform motion; for motion with acceleration, however, this will generate large errors.

Turning out attention to the fact that  $p/\rho = RT = a^2/\kappa$  ( $R$  is the gas constant,  $a$  is the speed of sound, and  $\kappa = c_p/c_v$  is the ratio of the heat capacities),

$$\frac{du}{dt} + \frac{a^2}{\chi} \varepsilon^2 \frac{\partial \ln p}{\partial x} + \frac{\mu mu}{\rho \chi} + \frac{m^2 u^2}{\lambda} = 0 \quad (1.13)$$

for an ideal gas. Let us denote  $c = a\varepsilon/\sqrt{\kappa}$  as the spread velocity of a disturbance in a porous medium. For the three-dimensional laminar seepage flow of an ideal gas, we then have

$$\frac{d\bar{u}}{dt} + c^2 \bar{\nabla} p + \frac{\mu m \bar{u}}{\chi} = 0. \quad (1.14)$$

It is still necessary to consider the energy equation along with Eqs. (1.3) and (1.14). Bearing in mind that three-dimensional resistance forces of the soil framework due to the soil's immobility do not perform work, we obtain

$$\rho m \cdot d \left( e + \frac{u^2}{2} \right) / dt = - \frac{\partial p m u}{\partial x}$$

for a one-dimensional flow. For an ideal gas,  $e = c_v T$ , if we consider  $c_v = \text{const}$ . Using (1.3) and (1.14) and bearing in mind that  $p = \rho RT$ , this equation is transformed to [6]

$$d [\ln p - \chi \ln \rho] / dt = (\chi - 1) \frac{\mathcal{P} u}{p m}$$

or

$$\frac{d \ln T}{dt} = \left( \frac{\chi - 1}{\chi} \right) \left\{ \frac{\partial \ln p}{\partial t} + \varepsilon^2 u \left( \frac{\partial \ln p}{\partial x} + \frac{\mu u}{p \chi} \right) \right\}. \quad (1.15)$$

For steady-state flows, the temperature change will be of the order of  $\varepsilon^2$ , so that  $dT/dt \approx 0$ . The temperature of the ideal gas during seepage must be considered constant when  $\varepsilon^2 \ll 1$ . The Joule effect is considered during the seepage of a real gas.

§2. Determination of  $\varepsilon^2$ . With a uniform flow, it is neither possible to distinguish between "Archimedes force" and the force of hydrodynamic resistance, nor to determine  $\varepsilon^2$ . For this purpose, it is necessary to investigate flows with acceleration. The most direct method of determining  $\varepsilon^2$  is to measure the spread velocity  $c$  of a disturbance in a seepage flow.

During the seepage of gas, the simplest steady-state nonuniform flow under the conditions mentioned above (see Fig. 1) can be used to determine  $\varepsilon^2$ . Such tests were conducted at the N. Ye. Zhukovskii Central Aero-Hydrodynamic Institute by Kurshin [7] on a series of sandstone specimens from different seams. These specimens were obtained and pretested to determine their porosity and permeability by L. B. Berman at the All-Union Scientific-Research and Design Institute for Marine Petroleum and Gas. The results of Kurlaev's study [8] in which data derived from these experiments were investigated and processed, are given below.

The steady flow of gas in a specimen will be nonuniform. The flow rate along the specimen is constant, but the density along its length in proportion to the pressure drop. Let  $q$  be the flow rate through a unit cross-sectional area

$$q = \rho mu. \quad (2.1)$$

Since  $q = \text{const}$  and  $T = \text{const}$  along the specimen,  $d \ln p = d \ln \rho = -d \ln u$ , and the equation of the change in the amount of motion is

$$u \frac{du}{dx} + c^2 \frac{d \ln p}{dx} + \frac{\mu mu}{\rho \lambda} + \frac{m^2 u^2}{\lambda} = 0.$$

Let us designate the reduced velocity by  $u/c = N$ . Then

$$\left( \frac{1}{N} - \frac{1}{N^3} \right) \frac{dN}{dx} + \frac{\mu m^2}{\rho \lambda} + \frac{m^2}{\lambda} = 0. \quad (2.2)$$

When  $N \rightarrow 1$ ,  $dN/dx \rightarrow \infty$ .

If  $p_I$  is the gas pressure in chamber I at the inlet to the specimen when  $x = 0$ , which is equal to the gas pressure  $p_1$  in the first row of pores in the specimen, and  $N_0$  is the corresponding reduced velocity, then

$$\ln \frac{N}{N_0} + \frac{1}{2N^2} \left[ 1 - \left( \frac{N}{N_0} \right)^2 \right] + m^2 \left( \frac{\mu}{\rho \lambda} + \frac{1}{\lambda} \right) x = 0. \quad (2.3)$$

Let us designate  $p_1/p = p_{II}/p = \beta$ . We have

$$q = \frac{mpu}{RT} = \frac{pmN\lambda c}{a^2} = \frac{p_1 m \sqrt{\kappa} N \varepsilon}{a \beta} = \frac{p_1 m \sqrt{\kappa} N_0 \varepsilon}{a} \quad (2.4)$$

so that  $N/N_0 = \beta$ . Equation (2.3) assumes the form

$$\ln \beta - \left( \frac{1}{2N^2} \right) [\beta^2 - 1] + m^2 \left( \frac{\mu}{\rho \lambda} + \frac{1}{\lambda} \right) x = 0.$$

Let  $p_2$  be the gas pressure in the last row of pores in the specimen. This pressure may differ significantly from  $p_{II}$  - the gas pressure in the chamber beyond the specimen (with the loss of a high velocity head  $\rho w^2/\alpha$  in the last row of pores in the specimen).

For a specimen with a length  $l$ , we have

$$\ln \beta_2 - \left( \frac{1}{2N^2} \right) [\beta_2^2 - 1] + m^2 \left( \frac{\mu}{\rho \lambda} + \frac{1}{\lambda} \right) l = 0, \quad (2.5)$$

where

$$\beta_2 = p_1/p_2; \quad N_2 = q\beta_2/\rho_1 mc. \quad (2.6)$$

When the pressure gradient  $p_I - p_{II}$  increases with a constant  $p_I$  and decreasing  $p_{II}$ ,  $\beta_2 = p_2/p_1$  will increase, and the flow rate  $q$  and velocity  $u$  will rise. Finally, the velocity, even at the end of the specimen, is compared in terms of magnitude with the velocity  $c$  for a certain value  $\beta_2 = \beta_*$ . As is readily confirmed, this corresponds to the maximum  $q$  as a function of  $\beta_2$ . In this case,  $N = 1$  in (2.5) and (2.6).

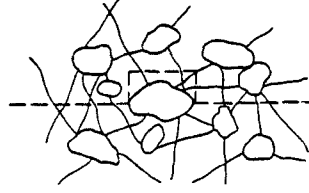


Fig. 10

With a further drop in the pressure  $p_{II}$ , the disturbances can no longer penetrate into the specimen (they will be blown away by the seepage flow encountered) and this pressure drop will no longer give rise to a change in the flow rate  $q$ . Let us designate the critical flow rate by  $q_*$  and  $\beta_*$  as the critical value of  $\beta$ . From (2.5),

$$\ln \beta_* - 0,5[\beta_*^2 - 1] + m^2 \left( \frac{\mu}{q_* \chi} + \frac{1}{\lambda} \right) = 0 \quad (2.7)$$

and

$$\varepsilon = \frac{aq_* \beta_*}{p_1 m \sqrt{\chi}}. \quad (2.8)$$

Measuring  $q_*$ , calculating  $\beta_*$  from  $p_I - p_{II}$ , and knowing  $m$ ,  $a$ ,  $\kappa$ , and  $p_1$ ,  $\varepsilon$  is determined from (2.8), and the term containing the resistance factors  $\chi$  and  $\lambda$  from Eq. (2.7).

The onset of the critical seepage regime is totally analogous to the familiar phenomenon observed during the outflow of gas from a convergent nozzle. When the velocity of outflow at the end of the nozzle in its narrowest cross section becomes equal to the speed of sound, the pressure drop in the chamber beyond the nozzle will no longer cause an increase in the flow rate of gas through the nozzle (St. Venant paradox). A similar phenomenon observed during seepage conforms, by nature, completely to this effect. The cessation of the increase in seepage flow is associated with the fact that the velocity  $w$  of the gas flow in the narrow sections of connected slits in the last row of pores becomes equal to the speed of sound  $w = a = a_*$ . Let  $f = \sum f_i$  be the total area of the critical cross sections of these slits, which belong to a unit of cross-sectional area and which are formed by soil grains that intersect the last section of the specimen (Fig. 10). Let the velocity vector  $\vec{w}_i$  in this slit in the critical section be the angle  $\phi_i$  with the direction of the seepage velocity; in this case,  $\phi_i$  may even be greater than  $\pi/2$ . The amount of gas passing through this slit per unit time in the direction of the seepage velocity is  $f_i a_* \rho_* \cos \phi_i$ , such that  $\rho_* a_* A f = \rho_0 c m$ , where

$A = \sum f_i \cos \phi_i / \sum f_i < 1$ ,  $c = a \varepsilon \sqrt{\chi}$ . Considering the flow in the slits prior to the critical section to be isentropic  $a_*/a_0 = \sqrt{2/(\kappa + 1)}$  and  $\rho_*/\rho_0 = (2/(\kappa + 1))^{1/(\kappa-1)}$ , we obtain

$$\varepsilon = A \sqrt{\frac{2\kappa}{\kappa + 1}} \left( \frac{2}{\kappa + 1} \right)^{1/(\kappa-1)} \cdot \frac{f}{m}. \quad (2.9)$$

In processing the experiments and determining  $\beta_*$ , attention should be focused primarily on the exhaust losses in the outlet section of the specimen. In narrow slits corresponding to the last row of dissected pores of the specimen, the velocity  $w$  for the critical regime is everywhere equal to the speed of sound, and this velocity at the outlet from the slits is virtually everywhere greater than the speed of sound for a nonuniform velocity distribution across the section of the specimen. The corresponding velocity head  $\rho a^2/2$  is completely lost, i.e., is not restored in pressure. If  $p_2$  is the pressure in the pores prior to the outlet section and  $p$  is the pressure in the narrowest section of the slits, we have, considering the flow at the inlet to the slit to be isentropic,

$$p_2/p = (1 + M^2(\kappa - 1)/2)^{\kappa/(\kappa-1)},$$

where  $M = w/a$ . When  $M = 1$ ,  $p/p_* = ((\kappa + 1)/2)^{\kappa/(\kappa-1)}$ . If the pressure in the outlet steam is not restored,

$$p_2 = p_{II} \left( (\kappa + 1)/2 \right)^{\kappa/(\kappa-1)} \quad (2.10)$$

for the critical regime;  $\kappa = 1.4$  for air, and  $p_2 \approx 1.90 p_{II}$  for the critical pressure.



At the end of the specimen, the pressure varies sharply, and the pressure gradient tends to infinity (see Fig. 2). The pressure distribution calculated for conditions where the inertial forces are neglected for a  $p_{II}$  corresponding to the critical pressure, and for  $p_{II} = 0$ , is also indicated by the broken line in Fig. 9.

The pressure gradient in the last row of pores is extremely large ( $p_2 - p_{II} = p_1/\beta_2 \cdot [1 - p_{II}/p_2]$ ) and for high  $p_I$  values, may lead to significant expansion and failure of the narrow slits in the last row of pores.

If the average value of these new narrow-slit sections that are formed is denoted by  $f_1$  and  $\epsilon_1$  is the corresponding value of  $\epsilon$ ,  $\epsilon_1/\epsilon = f_1/f$ . The value of this ratio may vary from specimen to specimen. A large pressure gradient may also lead to complete failure of at its end, and even to the development of a crushing wave, if a protective lattice is not established at the end of the specimen. Deformation of the specimen in its outlet section may increase the value of  $\epsilon_1$  severalfold in comparison with its actual value  $\epsilon$ .

Deformation of the soil framework with pressure variation in the pores of the specimen may also exert an influence on the spread velocity  $c$  of a disturbance in the specimen. This influence can be neglected for gas seepage; it is significant for the seepage of a liquid.

Data derived from the processing [8] of experiments conducted at the N. E. Zhukovskii Central Aero-Hydrodynamic Institute by Kurshin [7] for a series of specimens prepared from cores of various sandstones and specimens of an artificial porous material are presented below. Initial data on these specimens are given in Table 1.

TABLE 1. Initial Data on Specimens\*

Specimen number	m	K, mDc	l, m
Specimens from sandstone cores			
4	0.13	0.39	0.033
5	0.08	1.9	0.034
6*	0.24	137	0.037
7a	0.14	3.8	0.025
7	0.14	3.8	0.040
10a	0.13	2.6	0.028
10	0.13	2.6	0.049
11	0.20	220	0.055
12a	0.15	4.1	0.033
12	0.15	4.1	0.056
13a	0.24	460	0.032
13	0.24	460	0.062
14a	0.13	3.1	0.037
14	0.13	3.1	0.068
15a	0.16	80	0.038
Artificial material			
1A	0.20	5.2	0.02
2A	0.20	5.0	0.05

\*Specimens 6a-15a were bored out from specimens 6-15. The values of m and k were determined from the bored specimens.

TABLE 2. Measurement and Computational Data

Specimen number	$p_I$ , MPa	$q_w$ , kg/(m <sup>2</sup> ·sec)	$p_I/p_{II*} = 1.9 \cdot \beta_w$	$\epsilon \cdot 10^3$	$c$ , cm/sec
Sandstone-core specimens					
4	10	0.10	5	0.06	2
5	10	0.35	4	0.27	8
	5	0.15	4	0.23	7
6	10	5.2	4	1.3	38
	5	3.0	4	1.5	43
	2	1.4	4	1.8	52
	1	0.83	4	2.1	61
7a	10	1.1	4	0.48	14
	5	0.43	5	0.47	14
7	10	1.0	4	0.45	13
	5	0.36	5	0.40	12
	2	0.08	6	0.26	8
10a	10	0.82	5	0.48	14
	5	0.32	5	0.38	11
10	10	0.55	5	0.32	9
	5	0.18	5	0.21	6
11	10	18	4	5.5	160
	5	8.1	5	6.2	180
	2	2.4	6	5.5	160
	1	0.82	7	4.4	130
12a	10	1.1	5	0.56	16
	5	0.42	5	0.43	12
12	10	0.82	6	0.50	14
	5	0.30	6	0.37	10
13a	10	11	3	2.1	61
	5	5.5	3	2.1	61
	2	2	3	1.9	55
13	10	6.2	5	2.0	58
	5	2.9	5	1.8	52
14a	10	0.77	4	0.36	10
	5	0.31	4	0.30	9
14	10	0.12	4	0.06	2
15a	10	3.2	3	0.92	27
	5	1.4	3	0.80	23
	2	0.51	3	0.73	21
Artificial material					
1A	5	0.94	4.2	0.60	17
2A	5	0.411	8.6	0.54	16

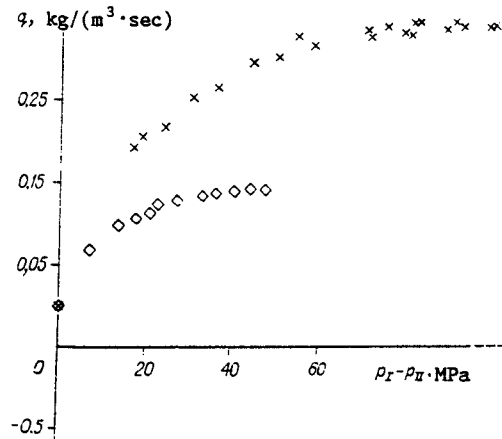


Fig. 11

Primary measurement data are presented as a relationship between the seepage flow rate  $q$  and the pressure gradient  $p_I - p_{II}$  in the chambers prior to and beyond the specimen. The measurement data for specimen No. 5 are given in Fig. 11.

For calculations, it is convenient to represent these data in the form of a curve of the dimensionless parameters  $q/q_*$  versus  $\beta$ . For this purpose, it is necessary to calculate the value of  $p_2$  from the measured values of  $p_{II}$ . For small  $M$  numbers, i.e., for pressure gradients significantly smaller than the critical,  $p_2 \approx p_{II}$ . When the regime is critical,  $p_2 = ((\chi + 1)/2)^{\chi/(\chi-1)} \cdot p_{II}$ . For intermediate  $M$  values, this ratio can be determined [8] from the equations

$$p_2/p_{II} = [1 + M^2(\chi - 1)/2]^{\chi/(\chi-1)},$$

$$q/q_* = M [1 - (1 - M^2)(\chi - 1)/(\chi + 1)]^{-(\chi+1)/2(\chi-1)}$$

or from corresponding tables in [9].

The relationship between  $q/q_*$  and  $p_I/p_{II}$  for specimen No. 5 is shown in Fig. 12; the corresponding computed curve for  $\chi = 0.03 \text{ mm}^2$ ,  $\lambda = 0.4 \text{ mm}$ , and  $p_I/p_{II*} = 1.9 \cdot \beta_* = 4$  is also shown here.

To determine the values of  $\chi$  and  $\lambda$  and to define  $\beta_*$  more precisely, they are selected so as to obtain the best correspondence between computational data and experimental relationship.

The  $q/q_* - \beta_2$  curve for all other specimens tested, with the exception of No. 6a, assumes the same character. Specimen No. 6a failed catastrophically at the end during testing.

The establishment of a critical flow rate and then its constancy over a broad range of variation in  $p_{II}/p_I$  are distinctly apparent in Fig. 12. The value of  $q_*$  is determined rather accurately from experimental data.

Since the speed of sound is different in the sections of the narrow slits that connect the pores, the flow rate is, as a result, stabilized only gradually with a drop in  $p_{II}$ . A more precisely defined value of  $\beta_*$  is obtained from comparison of the experimental and computed curves.

All sandstone specimens were first tested under an initial pressure of 10 MPa; this could have led to failure at their ends for the most brittle specimens.

Test and processed data for all specimens are presented in Table 2 from which it is apparent that the  $\epsilon_1^2$  value fluctuates from  $10^{-6}$  to  $10^{-9}$ . Tests with these same values of the ratio  $p_I/p_{II}$ , but for small  $p_1$  values should have been conducted to eliminate the possible effect of the end failure of the specimens and for more accurate determination of  $\epsilon^2$ .

§3. Liquid Seepage. Effect of Deformation of Soil Skeleton. During the nonsteady seepage of a liquid, when the relative change in the volume of the liquid as the pressure varies becomes comparable to the corresponding deformation of the pores, it is no longer possible to consider the porosity of the medium a constant that does not vary with the propagation of a seepage disturbance.

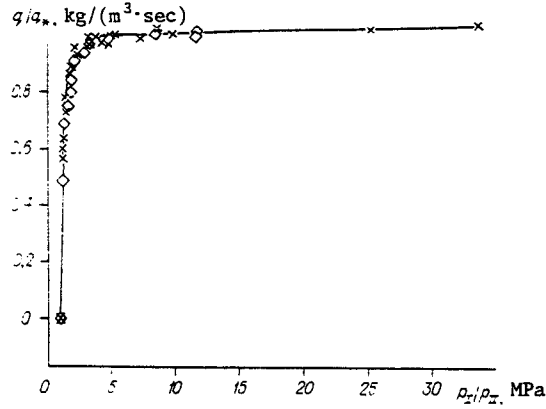


Fig. 12

Let us write the conservation equation, assuming that  $m = m(p)$ . Let the initial porosity when  $p = p_0$  be  $m_0 = m(p_0)$  over the entire space. For a one-dimensional flow, the equation of mass conservation with allowance for variation in porosity will be

$$d \ln \rho m / dt + \partial u / \partial x = 0. \quad (3.1)$$

The equation of state of the liquid, i.e., the equation relating the variation in density with the variation in its pressure and temperature (or entropy), is usually represented as

$$1 + p / \mathcal{P}_{00} = (\rho / \rho_0)^n. \quad (3.2)$$

where  $\mathcal{P}_{00} \approx 300$  MPa is the internal pressure of the liquid for water and the constant  $n = 7$ . The values of  $\mathcal{P}_{00}$  and  $n$  are functions of entropy. In a small temperature interval, however, they can be considered constants;  $\rho_0$  is the density at the initial temperature. From (3.2)

$$dp / d\rho = a_0^\alpha \cdot (\rho / \rho_0)^{n-1}; \quad a_0 = \sqrt{n \mathcal{P}_{00} / \rho_0}, \quad (3.3)$$

where  $a_0$  is the spread velocity of sound in the liquid.

Letting  $z = \ln(\rho / \rho_0)$ , we have [6]

$$p = \mathcal{P}_{00}[e^{nz} - 1] = n \mathcal{P}_{00} z [1 + nz/2 + \dots] \approx n \mathcal{P}_{00} z \quad (3.4)$$

from (3.2), and

$$dp / dz = n \mathcal{P}_{00} e^{nz} = n \mathcal{P}_{00} [1 + nz + \dots] \quad (3.5)$$

so that

$$d \ln \rho m = [1 + n \mathcal{P}_{00} e^{nz} d \ln m / dp] dz \quad (3.6)$$

or  $d \ln \rho m = [1 + B] dz$ , where [6]

$$B = n \mathcal{P}_{00} e^{nz} d \ln m / dp \approx n \mathcal{P}_{00} d \ln m / dp. \quad (3.7)$$

For a gas,  $B = \kappa p_0 d \ln m / dp$ , and  $\kappa p_0 / n \mathcal{P}_{00} \ll 1$ .

When the porosity varies with pressure, equation of mass conservation (3.1) will consequently be [6]:

$$[1 + B] dz / dt + \partial u / \partial x = 0. \quad (3.8)$$

The equation of the variation in the amount of motion with varying porosity will assume the form

$$\rho \frac{du}{dt} + \varepsilon^2 \frac{\partial p}{\partial x} + \frac{\mu m u}{\lambda} + \frac{\rho m^2 u^2}{\lambda} = 0. \quad (3.9)$$

The equation of variation in the amount of motion is

$$\frac{du}{dt} + \varepsilon^2 a_0^2 \frac{\partial z}{\partial x} + \frac{\mu m u}{\rho \lambda} + \frac{m^2 u^2}{\lambda} = 0. \quad (3.10)$$

It follows from Eqs. (3.8) and (3.11) that the spread velocity of a seepage disturbance in the porous medium with allowance for deformation of the soil skeleton  $D = \varepsilon a_0 / \sqrt{1 + B}$ .

To determine this velocity and compute the value of B, it is necessary to investigate the change in pore volume as a function of the pressure variation of the liquid in the pores.

Let us examine the change in pore volume as a function of the variation in their pressure with a constant external load on the soil skeleton, considering the deformation of the soil's framework to be elastic and neglecting inertial forces. The change in the volume of the pores as the pressure changes in them depends on their shape. A pore can always be approximated in the form of a certain ellipsoid, and the effect of a change in pore shape determined, comparing the deformations of the ellipsoids with different semi-axes from a sphere to a narrow slit (crack), which is an ellipsoid in planform with axes a and b and height  $\delta \ll a$ . Let us examine these two extreme shapes. For radial displacement in the vicinity of a spherical pore of radius a, which is located in an unbounded elastic space [12], we have

$$u_r = \frac{\sigma_\infty}{3\lambda + 2\mu} r + \frac{(p + \sigma_\infty)}{4\mu} \frac{a^3}{r^2}, \quad (3.11)$$

where  $\lambda$  and  $\mu$  are elastic constants,  $\sigma_\infty$  is the uniform compressive stress far from the pore, and r is a spherical coordinate with its center at the center of the pore. When p varies by  $\Delta p$  and  $\sigma_\infty$  is constant, we then have

$$\Delta u_r = \Delta p a / 4\mu$$

for the displacement on the surface of the pore. If the volume of the pore varies by the amount  $\Delta v = 4\pi a^2 \Delta u_r$ , the relative change in volume will be

$$\Delta v / v = 3\Delta p / 4\mu = 3(1 + \nu) \Delta p / 2E,$$

where E is Young's modulus and  $\nu$  is Poisson's ratio.

If the porosity is formed by spherical pores of different radii and is so small that the mutual effect of the pores on deformation can be neglected, then

$$\Delta m / m = \Sigma \Delta v / \Sigma v = 3(1 + \nu) \Delta p / 2E$$

and

$$d \ln m / dp = 3(1 + \nu) / 2E. \quad (3.12)$$

If the pore assumes the shape of a disk-like slit of radius a and height  $\delta$ , the increase in the volume of the pore as its pressure increases by  $\Delta p$  and for a constant  $\sigma_\infty$  will be [13, 14]

$$\Delta v = 16(1 - \nu^2) a^3 \Delta p / 3E$$

and

$$\Delta v / v = 4(1 - \nu^2) a \Delta p / \pi E \delta.$$

If the porosity is formed by disk-like cracks of different dimensions, but with a constant ratio  $\delta/a$ , we obtain

$$d \ln m / dp = 4(1 - \nu^2) a / \pi E \delta \quad (3.13)$$

by neglecting the mutual effect of the pores on their deformation.

In the Mathematics Department of the Novosibirsk Electrotechnical Institute, G. N. Mirenkova and E. G. Sosnina calculated in detail and compiled into tables and graphs the stresses and strains for a cavity in the shape of any form of ellipsoid to thin slits situated in an unbounded elastic space, and cited the relative changes in their volume as a function of pressure variation in the pores.

As is apparent, variation in porosity as a function of pressure variation in the pores depends very heavily on the shape of the pores. If, for example, the pressure in a pore varies by  $\Delta p = 10^2$  kgf/cm<sup>2</sup> when  $E = 10^5$  kgf/cm<sup>2</sup> and  $\nu = 0.3$ , the relative change in the volume of a spherical pore will be  $\Delta v / v = 0.2\%$ , and if this pore assumes the shape of a disk with  $\delta/a = 0.015$ ,  $\Delta v / v = 10\%$ .

Let us determine the spread velocity of a disturbance in a medium with a uniformly distributed porosity consisting of geometrically similar pores of the same configuration, for example, spherical pores or pores in the form of ellipsoids with the same ratio of principal axes, which are connected by the finest slits, the mass of the liquid in which is negligibly

small as compared with the mass of the liquid in the pores. In this case,  $d \ln m = dv/v$ , where  $v$  is the volume of one of the pores.

For spherical pores (3.12)

$$B = 3\mathcal{P}_{00}n(1+v)/2E,$$

and for a medium with cracklike pores (3.13)

$$B = 4(1-v^2)an\mathcal{P}_{00}/\pi E\delta.$$

If  $v = 0.13$ ,  $E = 10^5$  kgf/cm<sup>2</sup>, and  $\mathcal{P}_{00}n = 2 \cdot 10^4$  kgf/cm<sup>2</sup>,  $B = 0.4$  for a medium with spherical pores, and  $B = 24$  for a porous medium with cracks where  $a/\delta = 100$ .

If the shape and volume distributions of the pores are known such that it is possible to construct a corresponding distribution curve, the corresponding value of  $B$  is readily obtained by neglecting the mutual effect on their deformation. Let  $m = \Sigma m_i = \Sigma \alpha_i m$ , where  $\alpha_i$  is the percentage of pores of the same kind. However,  $\Delta m_i/m_i = A_i \Delta p$  and  $\Delta m = \Sigma \Delta m_i$ , and, consequently,  $\Delta m/m = \Sigma A_i \alpha_i \Delta p$  and  $B = \Sigma A_i \alpha_i n \mathcal{P}_{00}$ . Let, for example, the medium contain 25% of spherical pores, 50% of crack-like pores with  $a/\delta = 10$ , and 25% of pores with  $a/\delta = 100$ . Then,  $B = [0.25(1+v)3/2 + 0.5 \cdot 4(1-v^2)10/\pi + 0.25 \cdot 4(1-v^2)100/\pi]n\mathcal{P}_{00}/E$ ;  $B = 7$  when  $E = 10^5$  kgf/cm<sup>2</sup>,  $n\mathcal{P}_{00} = 2 \cdot 10^4$  kgf/cm<sup>2</sup>, and  $v = 0.3$ . If the deformation of the soil framework is inelastic, the wave-propagation process is related to the failure and irreversible deformations of the soil skeleton. The spread velocity of a seepage wave should then be determined with consideration of this process.

If  $m \ll 1$  and the pores are arranged in the volume such that the porosity is uniform, the influence exerted by pressure variation in one of the pores on the change in density in the vicinity of other pores can, as a rule, be neglected when  $\Delta p/E \ll 1$ . Let us assess the effect of the deformation of one pore on the deformation in the vicinity of another, which depends not only on the distance between these pores and their size, but also on the stiffness of the material in the soil framework (on the modulus  $E$ ).

Let the pressure in a spherical pore of radius  $a$  increase by  $\Delta p$ . The corresponding values of the projection of the pressure force on the surface of the hemisphere will be  $\pi a^2 \Delta p$  on the normal to the diametral section. The quantity  $r_0 = a\sqrt{(\pi \Delta p)/E}$  can be adopted as a measure of the distance determining the mutual effect between pores. Let the average distance between pores be equal to  $\ell$ . If  $r_0/\ell = \sqrt{\pi \Delta p/E} \cdot a/\ell \ll 1$ , the mutual effect of the pores is small, and we can neglect the change in density in the vicinity of one pore as the pressure varies in another. If the pores are a system of disk-like cracks of radius  $a'$  and thickness  $\delta$ , then

$$r'_0 = a' \sqrt{\pi \Delta p/E} \quad (3.14)$$

is a measure of the mutual effect of the cracks.

Let  $a$  be the radius of a spherical pore having the same volume as that of the disk-like crack. Then,  $a' = a\sqrt{a/\delta}$  and  $r'_0/r_0 = \sqrt{a/\delta}$ . If  $r'_0$  is of the order of unity or even higher, it is necessary to account for the mutual effect of the cracks to determine  $B$ .

§4. Transformation of Seepage Equations. Computational Example\*. Let us first examine a system of seepage equations in which the forces of hydrodynamic resistance are proportional to the seepage rate; this corresponds to Darcy's law.

Consideration of the effect of inertial forces leads to two constants - the "seepage-time scale"

$$t_0 = \rho_0 \chi / \mu m \quad (4.1)$$

and the spread velocity of a seepage disturbance  $c = a_0 \epsilon / \sqrt{k}$  for the seepage of a gas or  $D = a_0 \epsilon / \sqrt{1+B}$  for the seepage of a liquid in a porous elastic medium. The length  $\ell_0 = t_0 c$  or  $\ell_0 = t_0 D$  is then determined.

The equations of gas seepage in an isotropic medium assume the form

$$dz/dt + \bar{\nabla} u = 0, \quad d\bar{u}/dt + c^2 \bar{\nabla} h + \mu m \bar{u} / \rho \chi = 0, \quad (4.2)$$

where  $z = \ln(\rho/\rho_0)$ ,  $h = \ln(p/p_0)$ ,  $dz = dh$ . Assuming  $\vec{r} = \ell_0 \bar{R}$ , where  $\vec{v}$  is a radius vector,  $t = t_0 \tau$ ,  $u = c\bar{N}$ , equations (4.2) will assume the form

\*The results cited below were provided by A. R. Kurlaev.

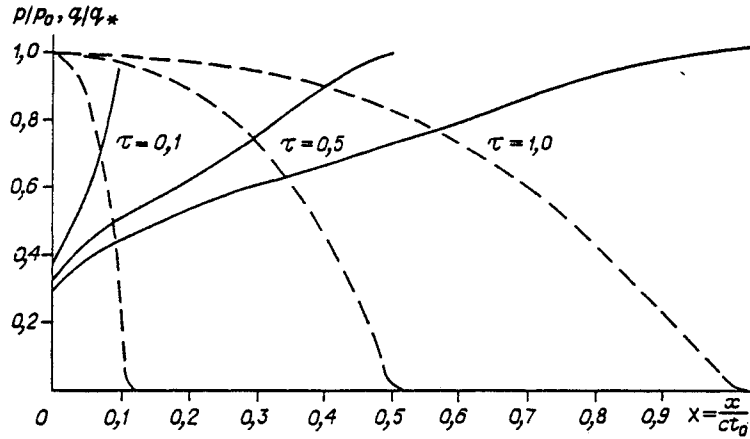


Fig. 13

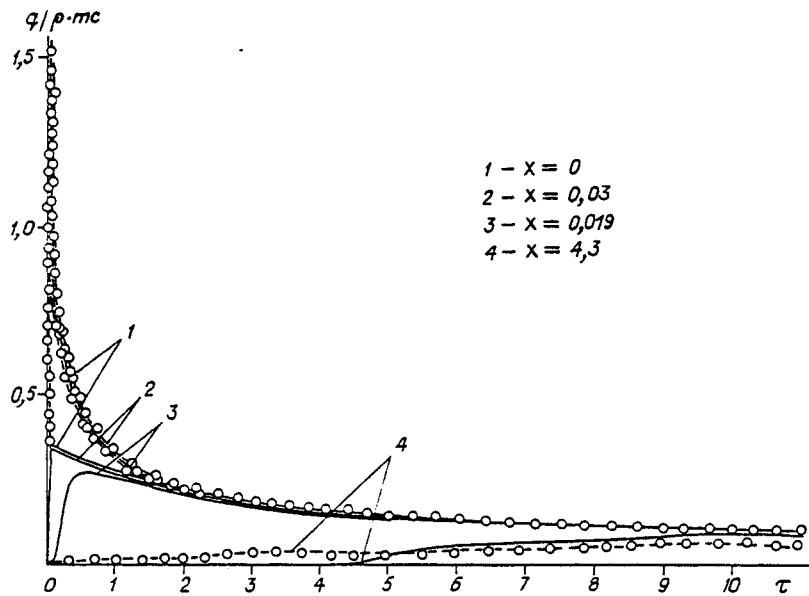


Fig. 14

$$\begin{aligned} \frac{\partial h}{\partial \tau} + (\bar{N} \cdot \bar{\nabla}) h + \bar{\nabla} \cdot \bar{N} &= 0, \\ \frac{\partial \bar{N}}{\partial \tau} + (\bar{N} \cdot \bar{\nabla}) \bar{N} + \bar{\nabla} h + e^{-h} \bar{N} &= 0. \end{aligned} \quad (4.3)$$

Setting  $z = (1 + B)Z$ , we obtain

$$\begin{aligned} \frac{\partial Z}{\partial \tau} + (\bar{N} \cdot \bar{\nabla}) Z + \bar{\nabla} \bar{N} &= 0, \\ \frac{\partial \bar{N}}{\partial \tau} + (\bar{N} \cdot \bar{\nabla}) \bar{N} + \bar{\nabla} Z + \bar{N} &= 0 \end{aligned} \quad (4.4)$$

for the seepage of a liquid. For a one-dimensional flow, these equations will assume, respectively, the form

$$\begin{aligned} \frac{\partial h}{\partial \tau} + N \frac{\partial h}{\partial X} + \frac{\partial N}{\partial X} &= 0, \\ \frac{\partial N}{\partial \tau} + N \frac{\partial N}{\partial X} + \frac{\partial h}{\partial X} + e^{-h} \cdot N &= 0 \end{aligned} \quad (4.5)$$

for the seepage of a gas ( $x = \lambda_0 X$ ), and

$$\begin{aligned} \frac{\partial Z}{\partial \tau} + N \frac{\partial Z}{\partial X} + \frac{\partial N}{\partial X} &= 0, \\ \frac{\partial N}{\partial \tau} + N \frac{\partial N}{\partial X} + \frac{\partial Z}{\partial X} + N &= 0 \end{aligned} \quad (4.6)$$

for the seepage of a liquid. Let  $\tau_0$  be the interval of dimensionless time in which the variation  $Z$  occurs. Let us set  $\tau = \tau_0 \eta$ . In Eqs. (4.5) and (4.6), the time derivatives will assume the form  $\tau_0^{-1} \partial \dots / \partial \eta$ . If  $\tau_0 \ll 1$ , the terms  $N$  and  $Ne^{-h}$  can be neglected as compared with  $\partial N / \partial \tau$ , and if  $N \ll 1$ ,  $N \partial N / \partial X$  and  $N \partial Z / \partial X$  can also be neglected in Eqs. (4.5) and (4.6). The seepage equations will agree with the equations of wave propagation in gas dynamics in the absence of viscous-friction forces. When  $\tau_0 \approx 1$ , these equations agree with the equations of the propagation of sound waves (acoustics equations) in a medium with high hydrodynamic resistance. If  $\tau_0 \gg 1$ , a small parameter appears for the time derivatives.

Results of the computation of a one-dimensional seepage flow that develops in a tube filled with a stagnant gas at a pressure  $p_0 = p_I$  and a temperature constant throughout the space under a sudden pressure variation of from  $p_I$  to  $p_{II} = 0.1 p_I$  on the free surface are given in Fig. 13. The instantaneous pressure profiles over the length of the specimen are indicated by the solid curves, and the instantaneous flow-rate profiles by the broken curves. For specimen No. 5 with a length of 3.4 cm,  $t_0 = 2.2$  sec,  $c = 8$  cm/sec, and  $l_0 = 18$  cm, the wave front will reach the initial section of the specimen after 0.4 sec. This corresponds to  $\tau = 0.19$ . A. P. Kurshin's direct measurement of the propagation time of a seepage disturbance that develops in chamber I prior to chamber II for this specimen yielded approximately the same spread velocity. For specimen No. 13 with a length of 6.2 cm,  $t_0 = 3.4$  sec,  $c = 58$  cm/sec, and  $l_0 = 200$  cm, the wave front will reach the initial section of the specimen after 0.11 sec; this corresponds to  $\tau = 0.03$ .

The variation in pressure and flow rate with time in sections generated by computer calculation from Eqs. (4.5) is shown in Fig. 14; the broken line with the circles indicates corresponding pressure and flow-rate values obtained by Kochina [16] where the effective inertial forces were neglected.

A comparison is made in Fig. 14 in dimensionless coordinates for the medium corresponding to specimen No. 5:  $m = 0.08$ ;  $k = 1.9$  mDc,  $\epsilon = 2.7 \cdot 10^{-4}$ , and  $p_0 = 10$  MPa for air; and also to specimen No. 13:  $m = 0.22$ ,  $k = 460$  mDc,  $\epsilon = 20 \cdot 10^{-4}$ , and  $p_0 = 10$  MPa.

#### LITERATURE CITED

1. V. I. Aravin, Field Investigations of Seepage [in Russian], Énergiya, Leningrad (1969).
2. N. N. Neprimerov, Three-Dimensional Analysis of Oil Recovery from Cooled Seams [in Russian], Kazan State Univ. (1978).
3. Yu. M. Molokovich, N. N. Neprimerov, V. I. Pikuza, and A. V. Shtanin, Relaxation Seepage [in Russian], Kazan State Univ. (1980).
4. S. A. Khristianovich, "Nonsteady flow of a soil mass containing pore gas under high pressure," Fiz.-Tekh. Probl. Razrab. Polezn. Iskop., No. 3 (1982).
5. G. I. Barenblatt, V. M. Entov, and V. M. Ryzhik, Movement of Liquids and Gases in Porous Media [in Russian], Nedra, Moscow (1984).
6. S. A. Khristianovich, "Nonsteady flow of liquid and gas in a porous medium subjected to sharp pressure variations with time or large porosity gradients," Fiz.-Tekh. Probl. Razrab. Polezn. Iskop., No. 1 (1985).
7. A. P. Kurshin and L. V. Guseva, "Experimental investigation of critical-outflow regimes during the seepage of air through specimens formed from cores of natural permeable rock subjected to various pressure gradients," Collection of Abstracts for Manuscripts Deposited in the All-Union Institute of Mining Information [in Russian], Issue 7, 1988.
8. A. R. Kurlaev, "Critical Gas-Seepage Regimes," Deformation and Failure of Materials [in Russian], Moscow (1981).
9. S. A. Khristianovich, V. G. Gal'perin, and M. D. Millionshchikov, Applied Gas Dynamics [in Russian], Izd. Akad. Nauk SSSR, Moscow (1948).
10. Yu. P. Zheltov and S. A. Khristianovich, "On the hydraulic fracturing of an oil pool," Izv. Akad. Nauk SSSR, Otd. Tekh. Nauk, No. 5 (1955).
11. K. Terzaghi, Theory of Soil Mechanics [Russian translation], Gosstroizdat, Moscow (1961).
12. A. Lyav, Mathematical Theory of Elasticity [Russian translation], Moscow-Leningrad (1985).
13. I. N. Sneddon, Fourier Transformations [Russian translation], IL, Moscow (1955).
14. G. I. Barenblatt, "Mathematical theory of equilibrium cracks formed during brittle failure," Zh. Prikl. Mekh. Tekh. Fiz., No. 4 (1961).
15. A. S. Vavakin and R. L. Salganik, "Effective elastic characteristics of bodies with isolated cracks, cavities, and rigid inhomogeneities," Izv. Akad. Nauk SSSR, Mekh. Tverd. Tela, No. 2 (1978).

16. P. Ya. Polubarinova-Kochina, "On one nonlinear equation in partial derivatives, encountered in seepage theory," Dokl. Akad. Nauk SSSR, 13, No. 6 (1948).

DEFORMATION PROPERTIES OF ROCK DURING SUBCRITICAL FAILURE

V. P. Skripka, A. V. Talonov, and  
B. M. Tulinov

UDC 539.375

Mathematical models of the deformation of rock in a nonuniform stress field, which are based on the theory of the elastoplastic dilatance deformation, are widely used in calculating the stability of components of underground structures, predicting mine shocks, and investigating the mechanical effect of a blast [1, 2].

Numerous experimental investigations indicate that subcritical failure of geomaterials, which is characterized by the development of a large number of microcracks, is observed even prior to the appearance of main cracks in loaded specimens [3, 4]. Models of media corresponding to a large number of isolated cracks can be used for a theoretical description of this process [5-7].

The purpose of the present study is to model numerically the subcritical failure of rock in a nonuniform stress field on the basis of the fissured-medium model proposed by Talonov and Tulinov [7].

1. Let us examine an element of a linearly elastic medium weakened by a large number of isolated cracks, which is subjected to external stress  $\sigma_{ik}$ . Using the crack-distribution function  $F(Y)$  for a set of determining parameters  $Y$  (dimensions, spatial orientation of the cracks), the variation in the macroscopic strain tensor of the given element of the medium is represented as [5-7]

$$\delta \varepsilon_{ik} = \delta \varepsilon_{ik}^0 + \frac{1}{2} \delta \int (n_i V_k + n_k V_i) F(Y) dY, \quad (1.1)$$

where  $\varepsilon_{ik}^0$  is the strain tensor of a solid linearly elastic medium,  $n_i$  are components of the normal unit vector to the surface of the crack, and  $V_i$  are components of the vector of the average jump in displacements of the crack edges, which can be determined from solution of the elastic-theory problem concerning the motion of the edges of an isolated crack in an external stress field.

The rocks were initially weakened by a large number of cracks, the development of which leads to failure of the mass when its stress-strain state changes. The following relationship proposed by Talonov and Tulinov [7] is used to describe the variation in the size of an isolated crack with time:

$$v = \begin{cases} 0 & K < K_{1c}, \\ v_0 \Phi(K) & K_{1c} \leq K < K_f, \\ v_0 & K \geq K_f, \end{cases} \quad (1.2)$$

where  $K = \sqrt{K_1^2 + (K_{1c} K_2 / K_{2c})^2}$ ,  $K_1$  and  $K_2$  are factors of the tensile- and longitudinal-shear-stress intensity, which characterize the peculiarities of the stresses in the terminal zone of the crack,  $K_f$  is the threshold of failure at the limiting velocity  $v_0$ ,  $\Phi(K) = C \exp(\alpha K)$  is for dry materials, and  $\alpha$ ,  $C$ ,  $K_{1c}$ , and  $K_{2c}$  are material constants.

Expression (1.1) is valid prior to the moment of multiple intersection of the cracks. Eremenko et al. [8] conducted an experimental investigation of the interaction and merging of

---

Engineering-Physics Institute, Moscow. Translated from Fiziko-Tekhnicheskie Problemy Razrabotki Poleznykh Iskopaemykh, No. 5, pp. 19-25, September-October, 1989. Original article submitted October 25, 1988.